10.2478/abm-2010-0046

Asian Biomedicine Vol. 4 No. 3 June 2010; 373-383

Original article

Ataxia telangiectasia mutated nuclear localization in head and neck cancer cells is PPP2R2B-dependent

Chotika Suyarnsestakorn[a,b], Thatchawan Thanasupawat[c], Kantima Leelahavanichkul[d], J. Silvio Gutkind[d], Apiwat Mutirangura[c]

[a]Inter-Department Program of BioMedical Sciences, Faculty of Graduate School Chulalongkorn University Bangkok 10330; [b]The National Center for Genetic Engineering and Biotechnology, National Science and Technology Development Agency, Pathumtani 12120; [c]Center for Excellence in Molecular Genetics of Cancer and Human Diseases, Department of Anatomy, Faculty of Medicine, Chulalongkorn University, Bangkok 10330, Thailand. [d]National Institutes of Health/NIDCR, Bethesda, MD 20892-4340, USA

Background: Protein phosphatase 2A (PP2A) has been implicated in radiation-induced activation of cellular responses, likely by its ability to regulate the autophosphorylation of the ataxia telangiectasia mutated (ATM) protein, a key molecule involved in the DNA damage response initiated by double-stranded DNA breaks. Interestingly, a hereditary defect in the PPP2R2B gene, which encodes the beta isoform of PP2A regulatory subunit B, causes autosomal dominant spinocerebellar ataxia 12, a clinical condition resembling that of ataxia telangiectasia patients. Moreover, PPP2R2B is significantly downregulated in many human cancers, including head and neck squamous cell carcinomas (HNSCCs).

Objective: Examine whether PPP2R2B regulates ATM function, thereby contributing to tumor progression due to the resulting defective DNA repair.

Methods: The roles of PPP2R2B were evaluated in irradiated HNSCC cell lines, $siRNA_{PPP2R2B}$ cells and okadaic acid treated cells. Expression of PPP2R2B was measured by microarray, Western blot analysis and real time quantitative rtPCR. ATM quantity and localization, ATM phosphorylation and γ-H2AX were determined by Western blot analysis and/or immunofluorescence assay. Clonogenic cell survival assay was performed to determine ionizing radiation sensitivity.

Results: PPP2R2B expression is reduced in multiple tumor types, including HNSCCs. Indeed, HNSCC cell lines that have lower PPP2R2B mRNA expression and $siRNA_{PPP2R2B}$ cells lower basal and radiation-induced levels of phosphorylated ATM and the consequent reduction in the levels of phosphorylation of the downstream ATM target, γ-H2AX. Depletion of PPP2R2B and inhibition of PP2A with okadaic acid resulted in limited ATM nuclear localization. Finally, $siRNA_{PPP2R2B}$ cells displayed enhanced sensitivity to death after radiation.

Conclusion: In HNSCCs, ATM nuclear localization is PPP2R2B dependent, and decreased PPP2R2B expression may result in limited ATM activation by preventing its nuclear accumulation and ATM-chromatin interaction. Therefore, decreased PPP2R2B expression in HNSCCs may contribute to genomic instability, cancer development and radiation sensitivity by limiting ATM functions.

Keywords: ATM, head, neck, nuclear localization, PPP2R2B, PP2A, SCA12, squamous cell carcinoma

Protein phosphatase 2A (PP2A) is a member of the Ser/Thr protein phosphatase family, which plays a role in several cellular processes, including gene expression, cell development, cell division and cell signal transduction [1-3]. The core PP2A complex is composed of a 65 kDa scaffold structural subunit [4], and a 36 kDa catalytic subunit ($PP2A_C$ or C subunit). The free catalytic C subunit has high activity but low

Correspondence to: Prof. Apiwat Mutirangura, Center for Excellence in Molecular Genetics of Cancer and Human Diseases, Department of Anatomy, Chulalongkorn University, Bangkok 10330, Thailand. Email: mapiwat@chula.ac.th

specificity [5]. Thus, this substrate-indiscriminate or non-specific activity of the C subunit must be regulated to prevent general dephosphorylation. The third PP2A subunit, the B subunit ($PP2A_B$), fills this need [1], and the $PP2A_B$, or B regulatory, family is the most variable group among the different subunit families. In theory, the multiple members of each subunit family can combine to form more than 72 distinct ABC trimeric complexes [6]. Thus far, four major classes of B subunits have been identified: B, B', B'' and B''' [2, 7]. Each of these four sub-classes has been described to have tissue-specific expression. The B family has been shown to be enriched in brain, whereas the B' and B'' families are found in heart, skeletal muscle and brain. The fourth family, B''', is thought to be localized to neuronal dendrites [8].

Recently, PP2A was shown to reverse phosphorylation of the ataxia telangiectasia mutated (ATM) protein [9]. It was found that ATM interacted constitutively with the A and C subunits of PP2A in undamaged lymphoblastoid cells. However, when cells were exposed to ionizing radiation (IR), the ATM and PP2A separated from each other and, consequently, ATM autophosphorylation occurred. Interestingly, Guo et al. [10] proposed a model in which IR activated ATM through a signaling pathway involving the dissociation of the regulatory B subunit alpha isoform (PPP2R2A) from heterotrimeric PP2A. Interestingly, spinocerebellar ataxia type 12 (SCA12), which is caused by the expansion of CAG triplet repeats within the promoter region of the PPP2R2B gene, shares characteristics with ataxia telangiectasia (A-T) syndrome, which is characterized by progressive neuronal degeneration and cerebellar ataxia [11-13]. The protein product of PPP2R2B, a PP2A regulatory B subunit beta isoform, PPP2R2B, is 70% homologous to PPP2R2A, and both subunits are found in the same sub-populations of neurons [14]. The similarity in the phenotypic manifestations of PPP2R2B and ATM genetic deficiencies prompted us to examine the possibility that PPP2R2B may regulate ATM function, therefore contributing to human malignancies characterized by genomic instability resulting from defective DNA repair.

Materials and methods

Cell culture

Head and neck squamous cell cancer (HNSCC) cells (WSU-HN) [15] were cultured in Dulbecco's modified Eagle's medium (DMEM; Gibco BRL, Life Technologies, Pairly, UK) supplemented with 10% heat-inactivated fetal bovine serum (Sigma, St. Louis,MO, USA). Cells were incubated at 37°C in 5% CO_2. To inhibit PP2A function by okadaic acid (OA), WSU-HN13 cells were treated with either 0.5 μM OA or 0.1% DMSO for 30 minutes. For the radiation treatment, cells were incubated in an ice-cold medium before exposure to 2.0 Gy γ-ray at a rate of 6.22 cGy/min with a ^{60}Co source (Eldorado 78).

Gene expression microarray

Gene expression microarray was performed to examine the mRNA expression profile of various B subunits of PP2A. Labeled cDNA targeted for hybridizations was synthesized by the Quick Amp kit (Agilent Technologies, Palo Alto, USA) from 800 ng of universal human reference and samples in the presence of CyTM3 and CyTM5 reactive dye, respectively. The labeled probes were hybridized with oligonucleotide microarrays (Agilent Technology, Palo Alto, USA) for 17 hours at 65°C. Hybridized slides were scanned by an Agilent Microarray scanner. The acquired image was analyzed and the intensity ratio of Cy™3 and Cy™5 was calculated by Feature Extraction software (Agilent Technologies, Palo Alto, USA).

Real-time reverse transcription polymerase chain reaction assay

Total RNA was extracted from WSU-HN cell lines using TRIzol®LS Reagent (Invitrogen, CA, USA), and first strand cDNA templates were prepared with the RevertAid™ first strand cDNA synthesis kit (Fermentas, Vilnius, Lithuania), as described by the manufacturer. The expression of PPP2R2B and glyceraldehyde-3-phosphate dehydrogenase (G3PDH) mRNA was detected by real-time PCR using a QuantiTect SYBR Green PCR Kit (Qiagen, Basel, Switzerland) and specific primers (PPP2R2B forward: 5'-GGACATTAAGCCAGCCAACA-3', PPP2R2B reverse: 5'-TCCCTGGTCATGATATACCTCC-3'; G3PDH forward: 5'-GTGGGCAAGGTCATCCCTG-3', G3PDH reverse: 5'-GATTCAGTGTGGTGGGG GAC-3'). All reactions were run on a Lightcycler instrument (Roche Applied Science). To control for cell background effects, the expression of PPP2R2B was normalized to the expression of G3PDH.

Stable small interfering RNA (siRNA) transfection

WSU-HN4 cells were stably transfected with siRNA against PPP2R2B mRNA. The oligonucleotide sequences of the siRNA targeting PPP2R2B were as follows: sense strand: 5- GATCCGCGTGATGT GACCCTAGGCTTCAAGAGAGCCTAGGGTCACA TCACGCTTTTTTGGAAA-3 and antisense strand: 5AGCTTTTCCAAAAAAGCGTGATGTGACCCT AGGCTCTCTTGAAGCCTAGGGTCACATCACG CG-3. The oligonucleotide was subcloned into the PsilencerTM 3.1 vector (Ambion, Austin, Texas, USA). The siRNA-containing expression vector and empty vector were then transfected into WSU-HN4 cells using siPORTTM XP-1 (Ambion, Austin, USA). Selection with 250 μg/ml hygromycin B (Roche) was initiated 24 hours after transfection. Stably transfected WSU-HN4 cells were obtained by three to four weeks after transfection. The $siRNA_{PPP2R2B}$ and $siRNA_{neg}$ cells were seeded for 24 hours in DMEM with 10% FBS at 37°C and 5% CO_2 before IR.

Western blot analysis and antibodies

After IR, medium was replaced with 37°C medium, and cells were further incubated at 37°C and 5% CO_2 for 0, 30, 60, 90, 120 and 180 minutes before harvesting. Harvested cells were lysed in lysis buffer (0.05 M Tris, pH 7.4; 1% SDS), boiled for 5 minutes, and then immediately placed on ice. Proteins were run on SDS-polyacrylamide gels and transferred to either polyvinylidene difluoride or nitrocellulose membranes. Antibodies were purchased as indicated: PPP2R2B monoclonal antibody (ABNOVA, Taipei, Taiwan), anti-phospho histone H2AX monoclonal antibody (Upstate, Charlottesville, USA), anti-G3PDH antibody (Trevigen, Gaithersburg, USA), anti-ATM (2C1) antibody (GeneTex, San Antonia, USA), anti-phospho ATM (Ser1981) monoclonal antibody (Upstate, Charlottesville, USA), horseradish peroxidase (HRP)-goat anti-rabbit IgG (H+L) conjugated (Zymed® Laboratories, San Francisco, USA) and goat anti-mouse IgG-HRP sc-2005 HRP conjugated (Santa Cruz Biotechnology). Signals were developed using the Supersignal west chemiluminescent substrate optimization kit (Pierce, Rockford, USA). Data were analyzed to determine band densities of PPP2R2B and G3PDH and ATM, ATMS1981p, γ-H2AX and G3PDH.

Transient small interfering RNA transfection

WSU-HN13 cells were transiently transfected with siRNA against PPP2R2B mRNA ($siRNA_{PPP2R2B}$), which was designed by and purchased from Thermo Scientific, Dhamacon. A nonsilencing siRNA with no homology to any known mammalian genes (AllStars negative control siRNA, QIAGEN, Basel, Switzerland) was transiently transfected as a negative control siRNA ($siRNA_{neg}$) for each experiment. Transfected cells were seeded at $1.5x10^5$ cells/60 mm^2 dish for 24 hours on uncoated 22x22 mm^2 cover glasses. Cells were then exposed to 2.0 Gy γ-ray and incubated further at 37°C and 5% CO_2 for 90 minutes before immunofluorescence staining.

Immunofluorescence microscopy

Media were aspirated and cells were washed twice with 1X PBS. Cells were fixed with 4% paraformaldehyde in 1X PBS at room temperature for 10 minutes and washed 3 times with 1X PBS. Cells were then lysed with 0.05% TritonX-100 in 1X PBS at room temperature for 10 minutes and washed 3 times with 1X PBS. To block non-specific binding of antibodies, 3% BSA in 1X PBS was added and incubated at room temperature for 30 minutes. Excess BSA was removed, and primary antibody diluted in 3% BSA in 1X PBS was added and incubated for 90 min at room temperature. Anti-PPP2R2B antibody was purchased from Upstate (Charlottesville,, USA). After primary antibody incubation, cells were washed 3 times with 1X PBS, and either Alexa Fluor 488 goat anti-mouse or Alexa Fluor 546 goat anti-rabbit (Invitrogen, USA) was added. Cells were incubated for one hour at room temperature without light and washed three times with 1X PBS. The cover glass was mounted with mounting medium with DAPI and edges were sealed with clear nail polish. The fluorescence signal was visualized and imaged using a Zeiss AxioImager Z1 microscope coupled to an ApoTome, using AxioVision 4.6 software.

Clonogenic cell survival assay

Both stable $siRNA_{PPP2R2B}$ and $siRNA_{neg}$ cells in the exponential growth phase were seeded at 200 cells per 100-mm tissue culture dish following IR treatment at 0, 1, 2, 3, 4, and 5 Gy γ-ray. After the 11^{th} passage, cells were fixed with 10% trichloroacetic acid for 30 minutes and washed 3 times with tap water. Cells were air dried, stained with 0.057% (w/v) sulforhodamine B for 10 minutes, and washed three times with 1% acetic acid. Colonies containing >50 cells were marked as survivors.

Statistical analysis

A one-way Spearman statistical analysis was used to assess the differences between the amounts of PPP2R2B mRNA and ATMS1981p or γ-H2AX (γ-H2AX and ATMS1981p band densities were normalized to GAPDH and total ATM, respectively), as well as the induction of ATMS1981p and γ-H2AX or ATM and ATMS1981p. Differences were considered significant if $p < 0.05$. Student t test was used to assess the differences between the amounts of ATM or ATMS1981p between $siRNA_{PPP2R2B}$ and $siRNA_{neg}$ cells.

Results

Expression of PPP2R2B in human cancers

We evaluated the expression status of PPP2R2B in a variety of human cancers by computational analysis of multiple gene array databases using Oncomine (*http://www.oncomine.org*) [16]. Surprisingly, PPP2R2B is significantly downregulated ($p < 0.01$) in many highly prevalent human cancers, including colon cancer, head and neck cancer, esophageal cancer, bladder cancer, melanoma, and brain tumors. Given that genomic instability is a frequent event in HNSCCs [17-19], we focused our attention on this aggressive cancer type [20]. From studies by Ginos et al. [21] and Pyeon et al. [22], PPP2R2B was shown to be significantly downregulated in HNSCCs, with these studies reporting p values of 8.8×10^{-5} and 2.1×10^{-3}, respectively. While PPP2R2B RNA levels may be important in HNSCC development, the biological role of this PP2A subunit has not yet been explored.

Correlations between PPP2R2B mRNA expression and ATMS1981p

We evaluated the regulatory B subunit expression in WSU-HN cells [15] by microarray expression analysis (**Fig. 1A**). A variation in PPP2R2B mRNA levels was observed (**Fig. 1A**). In order to examine whether there was an association between PPP2R2B mRNA expression and ATM activity, RNA and protein from WSU-HN cell lines were collected for real time quantitative RT-PCR and Western blot analysis, respectively. An antibody to ATMS1981p was used to determine the amount of phosphorylated ATM, which represents the active form of ATM upon DNA damage [23]. We also determined the amount of γ-H2AX, the serine 139-phosphorylated form of histone H2AX. γ-H2AX is a known downstream target of ATM, hence enabling us to monitor the functional activity of ATM [24]. Interestingly, there were significant and direct correlations between PPP2R2B mRNA expression and ATMS1981p and between PPP2R2B mRNA levels and γ-H2AX (**Fig. 1B**). Moreover, as expected, there was a significant correlation between ATMS1981p and γ-H2AX (**Fig. 1B**). P53 statuses of these cell lines were reported elsewhere [25]. We found that the correlation between PPP2R2B mRNA expression and ATMS1981p was not dependent on P53 mutation. For example, whereas WSU-HN 6 and WSU-HN30 express low level of PPP2R2B, only WSU-HN 6 has P53 mutation. Therefore, we concluded that PPP2R2B might affect ATM phosphorylation and, consequently, its activity in vivo reflected by the formation of γ-H2AX.

To further verify the role of PPP2R2B in ATM phosphorylation, siRNA technology was utilized to target PPP2R2B mRNA in WSU-HN4 cells using control siRNA as a control for transfection. As shown in Figure 2A, PPP2R2B protein was downregulated in $siRNA_{PPP2R2B}$ cells compared to those transfected with its control, $siRNA_{neg}$ cells. We examined the levels of phosphorylated ATM and γ-H2AX in $siRNA_{PPP2R2B}$ cells and $siRNA_{neg}$ cells after the induction of DNA double-strand breaks (DSBs) by IR. As shown in **Fig. 2B**, no ATMS1981p was detected in either cell line under basal conditions. However, the level of ATMS1981p in $siRNA_{neg}$ cells was immediately detected after IR (0 minute) and persisted until 180 minutes after IR, which was the last time point that we examined. In contrast, ATMS1981p was not detected immediately after IR in $siRNA_{PPP2R2B}$ cells, but ATM phosphorylation did increase gradually and was detectable 30 minutes after IR. For each time point between 30 and 180 minutes after IR, we measured the density of the ATMS1981p bands and found that band density was lower in the $siRNA_{PPP2R2B}$ cells compared to the $siRNA_{neg}$ cells at every time point. Additionally, γ-H2AX was detected to a lesser extent in $siRNA_{PPP2R2B}$ cells than in $siRNA_{neg}$ cells at each time point. These findings support a role of PPP2R2B in promoting ATM phosphorylation and, consequently, γ-H2AX formation.

Significant amounts of ATM protein can be found in both $siRNA_{PPP2R2B}$ and $siRNA_{neg}$ cells. Even though the amounts of ATMS1981p between $siRNA_{PPP2R2B}$ and $siRNA_{neg}$ cells were different ($p < 0.01$), the ATM protein was not ($p = 0.77$)

(**Fig. 2B**). Moreover, no correlation between the amounts of ATMS1981p and ATM were observed (r=0.01, p=0.97). Therefore, the reduced ATM phosphorylation in $siRNA_{PPP2R2B}$ did not depend on the quantity of ATM. To confirm the role of PPP2R2B in ATM phosphorylation, immunofluorescence microscopy was performed. As shown in **Fig. 3**, foci formation of ATMS1981p and γ-H2AX were induced after IR in $siRNA_{neg}$ cells but not $siRNA_{PPP2R2B}$ cells.

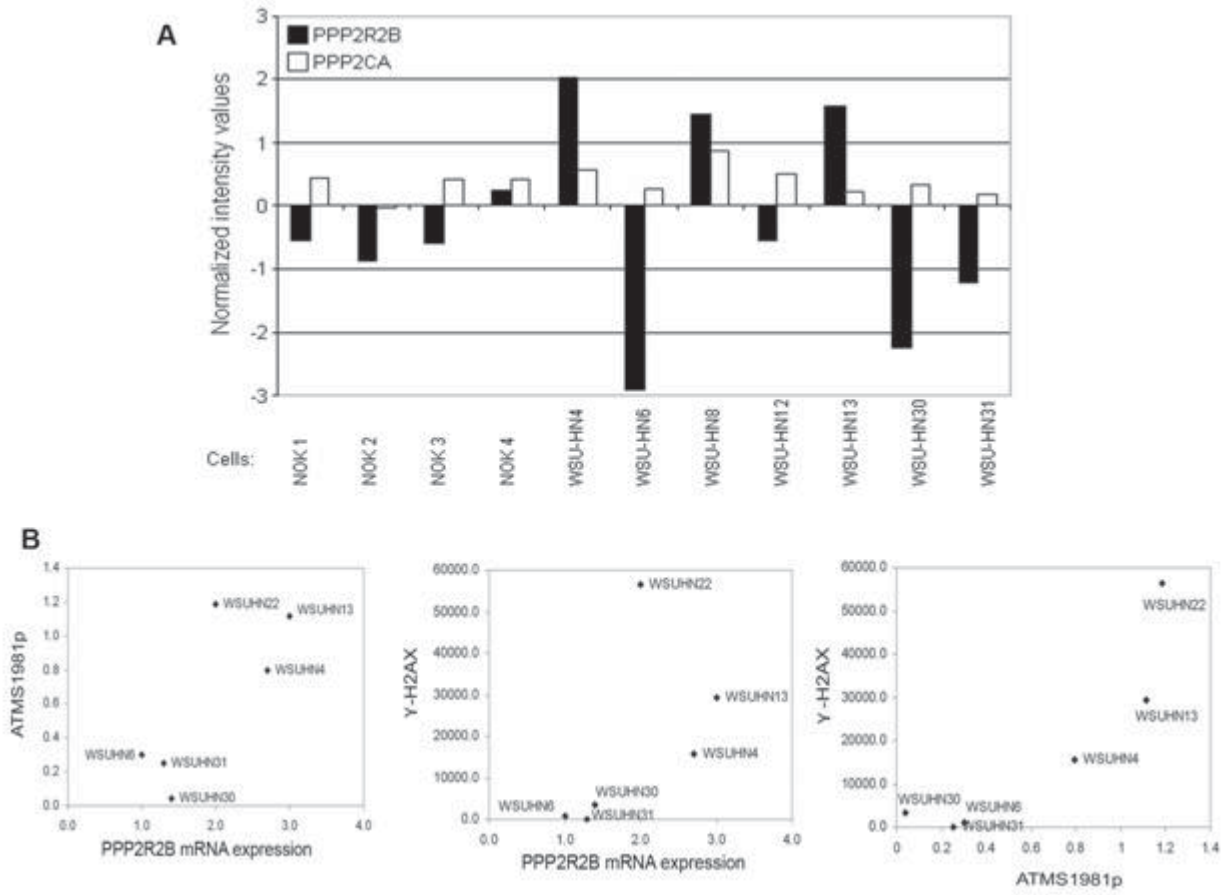

Fig. 1 The association between PPP2R2B mRNA and ATM phosphorylation levels. (**A)** A gene expression microarray was performed to examine the mRNA expression profile of various B subunits of PP2A. Normalized intensity values of PPP2R2B and PPP2CA were demonstrated. NOKs are normal oral keratinocytes and WSU-HNs are HNSCC cells. mRNA expression of PPP2R2B and glyceraldehyde-3-phosphate dehydrogenase (G3PDH) was detected by real-time PCR. (**B**) The association between PPP2R2B expression and either γ-H2AX or ATMS1981p levels, and the association between ATMS1981 and γ-H2AX in WSU-HN cells were analyzed. Spearman statistical analysis was used and all three associations were proven to be significant, with $p<0.05$.

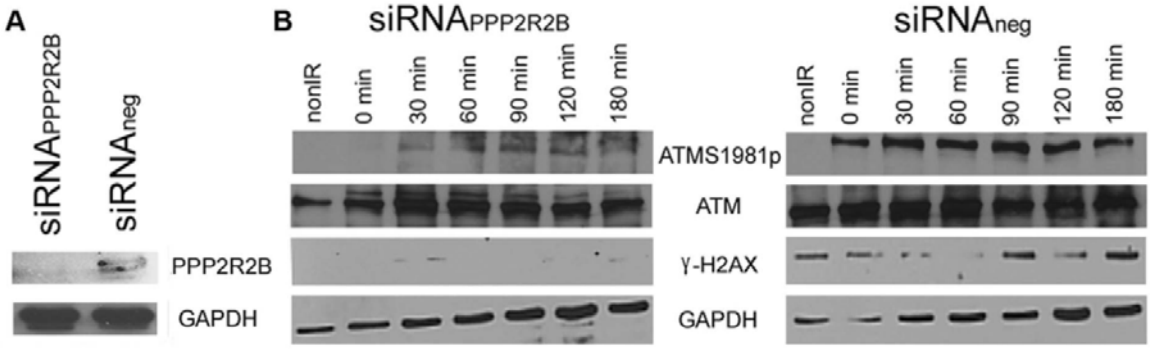

Fig. 2 Western blot of WSU-HN4 cells stably transfected with siRNA against PPP2R2B mRNA. (**A**) PPP2R2B and G3PDH and (**B**) ATM, ATMS1981p, γ-H2AX and G3PDH.

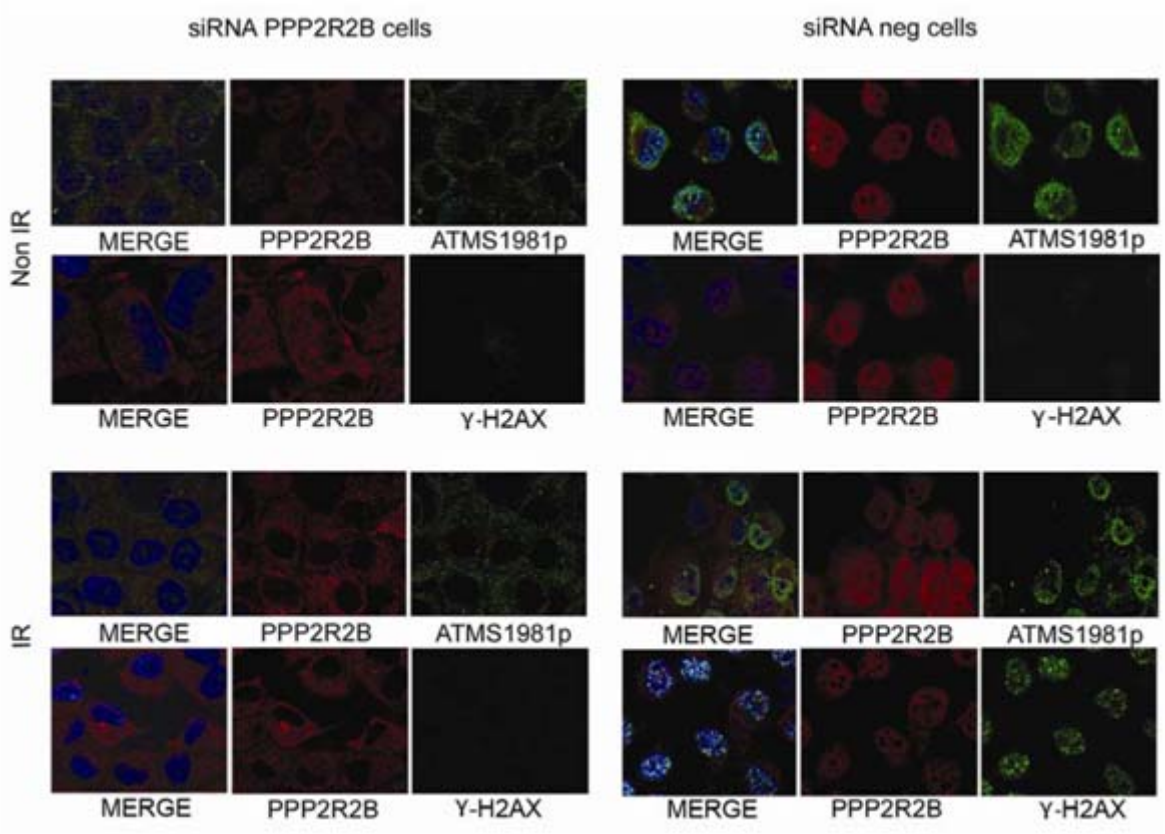

Fig. 3 The association between PPP2R2B mRNA and ATM phosphorylation levels by immunofluorescence. ATMS1981p and its downstream phosphorylation target, γ-H2AX, were investigated in WSUHN-13 cells transiently transfected with either siRNA against PPP2R2B mRNA or nonsilencing siRNA.

PPP2R2B and ATM localization

While evaluating ATM status, we were surprised to find that ATM of $siRNA_{PPP2R2B}$ cells was only localized within the cytoplasm and that IR did not result in ATM nuclear transport (Figure 4A). Recently, a nuclear localization sequence (NLS) was identified in ATM and mapped within its amino terminal [26]. Furthermore, interference of PP2A with OA, a specific inhibitor of PP2A, was shown to have an effect on nuclear localization of endogenous NLS-containing proteins [4]. We therefore investigated the role of the small molecule inhibitor of PP2A, OA, on ATM nuclear localization. Similar to $siRNA_{PPP2R2B}$ cells, ATM was found to be predominantly located within the cytoplasm of WSU-HN13 cells exposed to OA (**Fig. 4B**) in contrast to control cells, in which ATM was found distributed within both the cytoplasm and the nucleus (**Fig. 4B**). However, we found no evidence of ATM and PPP2R2B co-localization (**Fig. 4A**). Therefore, PPP2R2B may not directly form a protein complex with ATM. Our result suggests that PP2A plays a previously unknown function that ultimately controls ATM nuclear localization. Taken together, our finding reveals that PPP2R2B plays a significant role in promoting ATM nuclear localization. As chromatin interactions in the cell nucleus are a prerequisite for ATM autophosphorylation [27], either depleting PPP2R2B or its reduced expression in cancer cells may result in the inhibition of ATM activation by IR by preventing ATM nuclear localization. PPP2R2B and ionizing radiation sensitivity.

Phosphorylated ATM plays a key role in the regulation of cellular responses to IR and helps to rescue damaged cells [28]. Therefore, we were interested in investigating cell survival rates in both $siRNA_{PPP2R2B}$ and $siRNA_{neg}$ cells after IR exposure. For these studies, we used clonogenic cell survival assays, which can enable determination of the ability of cells to form colonies after exposure to IR or agents that lead to DSB induction. Specifically, we performed a clonogenic cell survival assay to compare the

radiation sensitivity of $siRNA_{PPP2R2B}$ and $siRNA_{neg}$ cells using a dose range of 1 to 5 Gy of radiation to provoke DSBs. As shown in **Fig. 5**, $siRNA_{PPP2R2B}$ cells, which lacked PPP2R2B, demonstrated a significant decrease in survival when compared to the survival of $siRNA_{neg}$ cells. These results demonstrate that cells without PPP2R2B are more sensitive to IR than cells with PPP2R2B expression, likely due to their inability to respond to DSBs and initiate the process of DNA repair.

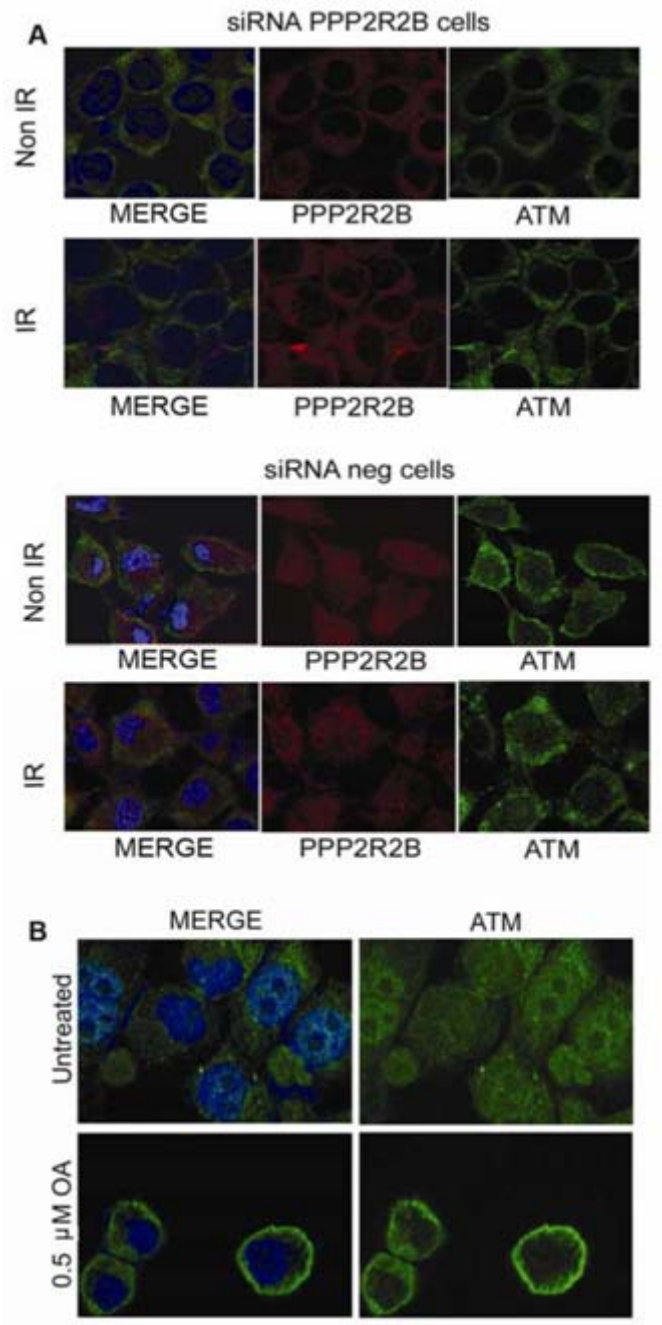

Fig. 4 Lack of PPP2R2B prevents ATM nuclear import. (**A**) WSUHN-13 cells were transiently transfected with either siRNA against PPP2R2B mRNA or nonsilencing siRNA, and immunofluorescence microscopy against PPP2R2B and ATM was performed. (**B**) Inhibiting PP2A by okadaic acid interferes with ATM nuclear import. WSU-HN13 cells were treated with either 0.5 μM OA or 0.1% DMSO. Cells were then harvested, and immunofluorescence microscopy against PPP2R2B and ATM was performed.

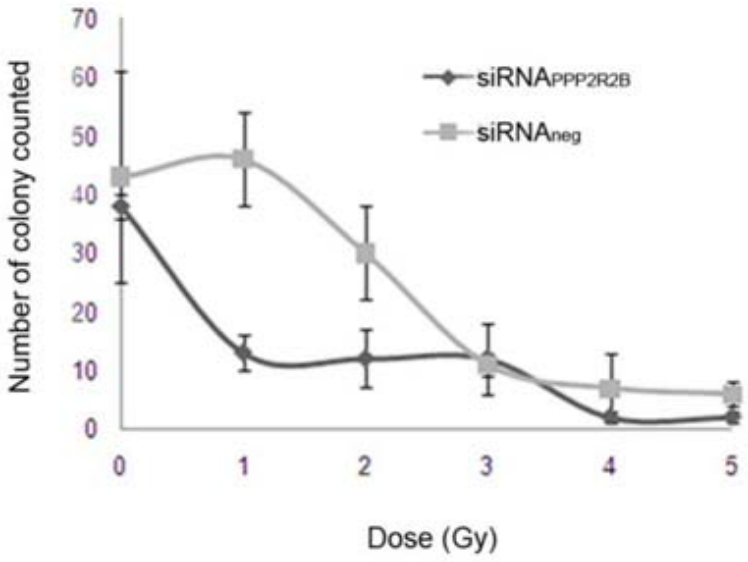

Fig. 5 Clonogenic cell survival assay reveals radiation sensitivity in $siRNA_{PPP2R2B}$ cells. Both $siRNA_{PPP2R2B}$ and $siRNA_{neg}$ cells were IR treated at 0, 1, 2, 3, 4 and 5 Gy γ-ray.

Discussion

Expression of PPP2R2B was found to be downregulated in many cancers, including HNSCC. Our experiments demonstrated that HNSCC cell lines that had lower PPP2R2B mRNA expression and $siRNA_{PPP2R2B}$ cells exhibited lower basal and radiation-induced levels of ATMS1981p, as well as its downstream phosphorylation target, γ-H2AX. Interestingly, $siRNA_{PPP2R2B}$ cells and HNSCC cells treated with OA in order to inhibit PP2A activity showed limited ATM nuclear localization. Finally, $siRNA_{PPP2R2B}$ cells showed a lower percentage of cell survival after radiation treatment than $siRNA_{neg}$ cells. Therefore, in HNSCCs, ATM nuclear localization has been shown to be PPP2R2B dependent, and the decrease in PPP2R2B expression appears to limit ATM activation by preventing ATM-chromatin interaction.

PPP2R2B and genomic instability

ATM plays an important role in maintaining genomic integrity [29]. Particularly in HNSCCs, ATM kinase is important in delta Np63 alpha phosphorylation/degradation after DNA damage [30]. Loss of ATM function has been shown to not only promote both inherited and sporadic cancers, but also increase radiosensitivity [31, 32]. Moreover, partial loss of genes, including ATM, has been shown to increase chromosomal instability after IR in HNSCCs [33]. The ATM/p53 pathway is proposed to be inactivated in HNSCCs by a number of distinct mechanisms [34]. ATM promoter hypermethylation was demonstrated in a quarter of HNSCCs [35]. Here, we show that cells with decreased PPP2R2B expression have reduced ATM function by inhibiting its nuclear localization. As the PPP2R2B subunit is significantly downregulated in HNSCCs [21, 22], it is reasonable to hypothesize that PPP2R2B expression is necessary for HNSCC cells to repair DSBs, hence maintaining genomic integrity. Consequently, a decrease in PPP2R2B expression might contribute to HNSCC genomic instability.

PPP2R2B and radiation sensitivity

Radiation therapy failure is a significant problem in cancer treatment. ATM promoter hypermethylation may be a marker of several tumors, indicating high radiosensitivity [36, 37]. Reducing ATM function by antisense inhibition enhances the radiosensitivity of cancer cells [38]. Here, we showed the variability of PPP2R2B expression in HNSCCs, in which the lower level of PPP2R2B expression may consequently limit ATM function. It is interesting and important to explore further if the expression of PPP2R2B is correlated with tumor radiosensitivity in vivo. Our experiments proved that the downregulation of PPP2R2B by siRNA might increase cell radiosensitivity. Similar to antisense ATM treatment, targeting PPP2R2B may be useful in order to improve tumor response to radiation therapy.

SCA12

Our observations regarding the role of PPP2R2B in regulating ATM function may have broader implications. For example, SCA12 patients have a PPP2R2B gene defect and a similar phenotype to A-T syndrome [11-13]. Based on the emerging results, we can speculate that the lack of PPP2R2B may phenocopy ATM deficiency due to the inability of ATM to be recruited to DSBs in the nucleus. Indeed, it should be intriguing to determine the relationship between SCA12 pathogenesis and ATM nuclear localization.

γ-H2AX

In cancer, γ-H2AX detection has been used to determine the extent of DSB induction [39, 40]. Consequently, γ-H2AX may represent an important marker to determine the presence of precancerous cells and, thus, of cancer staging [40]. More commonly, γ-H2AX is a crucial marker to detect genomic damage and is useful to monitor cancer treatment, particularly radiotherapy [41]. However, a decrease in expression of PPP2R2B would indirectly reduce γ-H2AX and the extent of DSBs would be underestimated. Therefore, our findings suggest that the expression level of PPP2R2B should be taken into consideration when the presence of γ-H2AX is used to determine the extent of DNA breaks.

Protein nuclear localization and cancer

One report demonstrated the role of PP2A on protein nuclear localization in cancer development. That is regulation of nuclear localization of GLI3, which controls transcription of various genes involved in cell growth and cell proliferation such as cyclin D1, through PP2A, its regulatory subunit, $^{\alpha}4$ [42]. This study shows tumor suppressor activity of PP2A and suggested anticancerogenic effects of rapamycin. From our study, PPP2R2B-involved PP2A was shown to inhibit ATM nuclear localization in HNSCCs. Our data suggests not only the role of PPP2R2B as a marker for monitoring but also the possibility that PP2A inhibitor enhances HNSCC radiation sensitivity.

Conclusion

PPP2R2B expression is reduced in multiple tumor types, including HNSCC. HNSCC cells that have lower PPP2R2B mRNA expression and HNSCC cells in which this gene was knocked down using specific siRNAs exhibited lower basal and radiation-induced levels of phosphorylated ATM, and the downstream ATM-target, γ-H2AX. Depletion of PPP2R2B and inhibition of PP2A with okadaic acid resulted in limited ATM nuclear localization. Finally, $siRNA_{PPP2R2B}$ cells displayed enhanced sensitivity to die after radiation. Therefore, in HNSCC, ATM nuclear localization is PPP2R2B dependent and that decreased PPP2R2B expression may result in limited ATM activation by preventing its ATM-chromatin interaction. Ultimately, these findings may suggest that decreased PPP2R2B expression in HNSCC may contribute to genomic instability and cancer development by limiting ATM function.

Abbreviation

A-T: ataxia telangiectasia,
ATM: ataxia telangiectasia mutated,
DSBs: DNA double-strand breaks,
G3PDH: glyceraldehyde-3-phosphate dehydrogenase,
HNSCCs: head and neck squamous cell carcinomas,
IR: ionizing radiation,
PP2A: protein phosphatase 2A,
OA: okadaic acid,
PPP2R2A: the regulatory B subunit alpha isoform from heterotrimeric PP2A,
PPP2R2B: the regulatory B subunit beta isoform from heterotrimeric PP2A,
siRNA: small interfering RNA,
SCA12: spinocerebellar ataxia type 12,
WSU-HN: HNSCC cell lines.

Acknowledgements

This study was supported by the Thailand Research Funds and the 90th Anniversary of Chulalongkorn University Fund (Ratchadaphisek-somphot Endowment Fund). C Suyarnsestakorn was supported by the Royal Golden Jubilee Ph.D. grant. KL and JSG were supported by the Intramural Program of the National Institute of Dental and Craniofacial Research, National Institutes of Health.

Authors declare no conflict of interest.

References

1. Janssens V, Goris J. Protein phosphatase 2A: a highly regulated family of serine/threonine phosphatases implicated in cell growth and signalling. Biochem J. 2001; 353(Pt 3):417-39.
2. Janssens V, Goris J, Van Hoof C. PP2A: the expected tumor suppressor. Curr Opin Genet Dev. 2005; 15: 34-41.
3. Schonthal AH. Role of serine/threonine protein

phosphatase 2A in cancer. Cancer Lett.2001; 170:1-13.
4. Lubert EJ, Sarge KD. Interaction between protein phosphatase 2A and members of the importin beta superfamily. Biochem Biophys Res Commun. 2003; 303:908-13.
5. Lad C, Williams NH, Wolfenden R. The rate of hydrolysis of phosphomonoester dianions and the exceptional catalytic proficiencies of protein and inositol phosphatases. Proc Natl Acad Sci USA. 2003; 100:5607-10.
6. Virshup DM. Protein phosphatase 2A: a panoply of enzymes. Curr Opin Cell Biol. 2000; 12:180-5.
7. Eichhorn PJ, Creyghton MP, Bernards R. Protein phosphatase 2A regulatory subunits and cancer. Biochim Biophys Acta. 2009; 1795:1-15.
8. Nakada N, Kuroda K, Kawahara E. Protein phosphatase 2A regulatory subunit Bbeta promotes MAP kinase-mediated migration of A431 cells. Cell Physiol Biochem. 2005; 15:19-28.
9. Goodarzi AA, Jonnalagadda JC, Douglas P, Young D, Ye R, Moorhead GB, et al. Autophosphorylation of ataxia-telangiectasia mutated is regulated by protein phosphatase 2A. Embo J. 2004; 23:4451-61.
10. Guo CY, Brautigan DL, Larner JM. ATM-dependent dissociation of B55 regulatory subunit from nuclear PP2A in response to ionizing radiation. J Biol Chem. 2002; 277:4839-44.
11. Holmes SE, O'Hearn EE, McInnis MG, Gorelick-Feldman DA, Kleiderlein JJ, Callahan C, et al. Expansion of a novel CAG trinucleotide repeat in the 5' region of PPP2R2B is associated with SCA12. Nat Genet.1999; 23:391-2.
12. Holmes SE, O'Hearn E, Margolis RL. Why is SCA12 different from other SCAs? Cytogenet Genome Res. 2003; 100:189-97.
13. Chun HH, Gatti RA. Ataxia-telangiectasia, an evolving phenotype. DNA Repair (Amst). 2004; 3: 1187-96.
14. Strack S, Zaucha JA, Ebner FF, Colbran RJ, Wadzinski BE. Brain protein phosphatase 2A: developmental regulation and distinct cellular and subcellular localization by B subunits. J Comp Neurol.1998; 392: 515-27.
15. Cardinali M, Pietraszkiewicz H, Ensley JF, Robbins KC. Tyrosine phosphorylation as a marker for aberrantly regulated growth-promoting pathways in cell lines derived from head and neck malignancies. Int J Cancer. 1995; 61:98-103.
16. Rhodes DR, Yu J, Shanker K, Deshpande N, Varambally R, Ghosh D, et al. ONCOMINE: a cancer microarray database and integrated data-mining platform. Neoplasia. 2004; 6:1-6.
17. Fan CY. Genetic alterations in head and neck cancer: interactions among environmental carcinogens, cell cycle control, and host DNA repair. Curr Oncol Rep. 2001; 3:66-71.
18. Wiseman SM, Stoler DL, Anderson GR. The role of genomic instability in the pathogenesis of squamous cell carcinoma of the head and neck. Surg Oncol Clin N Am. 2004; 13:1-11.
19. Richards KL, Zhang B, Baggerly KA, Colella S, Lang JC, Schuller DE, et al. Genome-wide hypomethylation in head and neck cancer is more pronounced in HPV-negative tumors and is associated with genomic instability. PLoS One. 2009; 4:e4941.
20. Subbalekha K, Pimkhaokham A, Pavasant P, Chindavijak S, Phokaew C, Shuangshoti S, et al. Detection of LINE-1s hypomethylation in oral rinses of oral squamous cell carcinoma patients. Oral Oncol. 2009; 45:184-91.
21. Ginos MA, Page GP, Michalowicz BS, Patel KJ, Volker SE, Pambuccian SE, et al. Identification of a gene expression signature associated with recurrent disease in squamous cell carcinoma of the head and neck. Cancer Res. 2004; 64:55-63.
22. Pyeon D, Newton MA, Lambert PF, den Boon JA, Sengupta S, Marsit CJ, et al. Fundamental differences in cell cycle deregulation in human papillomavirus-positive and human papillomavirus-negative head/neck and cervical cancers. Cancer Res. 2007; 67: 4605-19.
23. Bakkenist CJ, Kastan MB. DNA damage activates ATM through intermolecular autophosphorylation and dimer dissociation. Nature. 2003; 421:499-506.
24. Burma S, Chen BP, Murphy M, Kurimasa A, Chen DJ. ATM phosphorylates histone H2AX in response to DNA double-strand breaks. J Biol Chem. 2001; 276: 42462-7.
25. Yeudall WA, Jakus J, Ensley JF, Robbins KC. Functional characterization of p53 molecules expressed in human squamous cell carcinomas of the head and neck. Mol Carcinog. 1997; 18:89-96.
26. Young DB, Jonnalagadda J, Gatei M, Jans DA, Meyn S, Khanna KK. Identification of domains of ataxia-telangiectasia mutated required for nuclear localization and chromatin association. J Biol Chem. 2005; 280: 27587-94.
27. Kim YC, Gerlitz G, Furusawa T, Catez F, Nussenzweig A, Oh KS, et al. Activation of ATM depends on chromatin interactions occurring before induction of

DNA damage. Nat Cell Biol. 2009; 11:92-6.
28. Kurz EU, Lees-Miller SP. DNA damage-induced activation of ATM and ATM-dependent signaling pathways. DNA Repair (Amst). 2004; 3:889-900.
29. Shiloh Y. ATM and related protein kinases: safeguarding genome integrity. Nat Rev Cancer. 2003; 3:155-68.
30. Huang Y, Sen T, Nagpal J, Upadhyay S, Trink B, Ratovitski E, et al. ATM kinase is a master switch for the Delta Np63 alpha phosphorylation/degradation in human head and neck squamous cell carcinoma cells upon DNA damage. Cell Cycle. 2008; 7:2846-55.
31. Meyn MS. Ataxia-telangiectasia, cancer and the pathobiology of the ATM gene. Clin Genet. 1999; 55: 289-304.
32. Garcia MJ, Benitez J. The Fanconi anaemia/BRCA pathway and cancer susceptibility. Searching for new therapeutic targets. Clin Transl Oncol. 2008; 10:78-84.
33. Parikh RA, White JS, Huang X, Schoppy DW, Baysal BE, Baskaran R, et al. Loss of distal 11q is associated with DNA repair deficiency and reduced sensitivity to ionizing radiation in head and neck squamous cell carcinoma. Genes Chromosomes Cancer. 2007; 46:761-75.
34. Bolt J, Vo QN, Kim WJ, McWhorter AJ, Thomson J, Hagensee ME, et al. The ATM/p53 pathway is commonly targeted for inactivation in squamous cell carcinoma of the head and neck (SCCHN) by multiple molecular mechanisms. Oral Oncol. 2005; 41:1013-20.
35. Ai L, Vo QN, Zuo C, Li L, Ling W, Suen JY, et al. Ataxia-telangiectasia-mutated (ATM) gene in head and neck squamous cell carcinoma: promoter hypermethylation with clinical correlation in 100 cases. Cancer Epidemiol Biomarkers Prev. 2004; 13:150-6.
36. Kim WJ, Vo QN, Shrivastav M, Lataxes TA, Brown KD. Aberrant methylation of the ATM promoter correlates with increased radiosensitivity in a human colorectal tumor cell line. Oncogene. 2002; 21:3864-71.
37. Roy K, Wang L, Makrigiorgos GM, Price BD. Methylation of the ATM promoter in glioma cells alters ionizing radiation sensitivity. Biochem Biophys Res Commun. 2006; 344:821-6.
38. Zou J, Qiao X, Ye H, Yang Y, Zheng X, Zhao H, et al. Antisense inhibition of ATM gene enhances the radiosensitivity of head and neck squamous cell carcinoma in mice. J Exp Clin Cancer Res. 2008; 27:56.
39. Rogakou EP, Pilch DR, Orr AH, Ivanova VS, Bonner WM. DNA double-stranded breaks induce histone H2AX phosphorylation on serine 139. J Biol Chem. 1998; 273:5858-68.
40. Bonner WM, Redon CE, Dickey JS, Nakamura AJ, Sedelnikova OA, Solier S, et al. GammaH2AX and cancer. Nat Rev Cancer. 2008; 8:957-67.
41. Kuo LJ, Yang LX. Gamma-H2AX - a novel biomarker for DNA double-strand breaks. In Vivo. 2008; 22:305-9.
42. Krauss S, Foerster J, Schneider R, Schweiger S. Protein phosphatase 2A and rapamycin regulate the nuclear localization and activity of the transcription factor GLI3. Cancer Res. 2008; 68:4658-65.